ADVANCED FUNCTIONAL MATERIALS
www.afm-journal.de

Invisible Photonic Prints Shown by Deformation

*Siyun Ye, Qianqian Fu, and Jianping Ge**

Invisible photonic prints shown by deformation are prepared by soaking the mechanochromic photonic paper with crosslinker (PEGDA) and subsequently crosslinking part of the paper through a photo lithography process. The key point of this new technique is creating patterns and background with very close photonic structures but different mechanochromic capabilities, so that the invisible photonic patterns in relaxed state can be revealed under deformation due to the nonuniform change in photonic structure. Based on the relationship between crosslinking level and the reflection changes during deformation, one can conclude that a low crosslinking level favors the hiding of invisible patterns and a high crosslinking level favors the showing of patterns. The as-prepared samples can instantly and reversibly show the patterns by deformation and hide them by relaxation for many times, and the encapsulation by PDMS rubber prolongs its life time and enhances its durability in practical usages. The current printing technique is capable of creating invisible photonic prints in both macroscale and microscale range, which makes them potentially useful for security and antifraud applications in daily life.

1. Introduction

Responsive photonic crystals (RPC) and photonic crystal (PC) based printing are two hot topics in intersection of chemistry and material science. Responsive photonic crystals, as a series of new material which changes its structure colors under external stimulus,[1] has attracted great interests due to the potential applications in colorimetric sensors for detecting physical,[2] chemical,[3] and biological changes,[4] antiglare displays,[5] encryption and security devices,[6] optical enhancement,[7] photo catalysis[8] and solar cells.[9] While the photonic printing, as a fundamental technique to integrate the aforementioned functions into practical photonic devices, has also been extensively investigated based on the direct self-assembly of colloidal crystals on substrate[10] or spatially tuning part of the photonic structure in a preformed photonic paper.[11]

The "invisible photonic prints" is a successful demonstration to the integration and further development of RPCs and PC printing techniques. Unlike the traditional photonic prints with an unchangeable pattern, the invisible photonic prints shall be unseen under normal circumstances, but can be recognized by specific methods later. It possesses characteristics of RPC since the invisible patterns are revealed by tuning the photonic structures. On the other hand, it behaves as a typical photonic print with recordable information and self-maintained patterns of structure colors. The main difficulty for invisible photonic prints is the creation of "pattern" and "background" with different response to the external stimuli but very close photonic structure at normal state, which seems to be contradictory in most cases. Therefore, although many printing methods and responsive photonic materials have been demonstrated in the past years, the fabrication of invisible photonic prints is still a big challenge.

Recently, we have reported an invisible photonic print shown by water.[12] Since the pattern and background sections on polymeric photonic paper have different swelling capabilities, their small difference in reflection wavelength (λ) was significantly amplified due to different swelling speed, which leads to a visible image after being soaked in water for several minutes. Later, an invisible photonic print shown by magnetic field was prepared by selectively drying the glycol content of magnetically tunable PCs in polydimethylsiloxane rubber.[13] When the sample is exposed to the magnetic field, part of them show structural color due to magnetic assembly of PCs while the rest maintain the color of magnetite due to losing the ability of assembly in magnetic field, which leads to the appearance of invisible pattern in the end.

In this work, a new member will join the family of invisible photonic prints, which shows the hidden patterns by deformation instead of water soakage or magnetic field. Thanks to the controlled assembly of metastable colloidal crystalline array (CCA)[14] in organic solvents including acrylate monomers, we are able to prepare the mechanochromic photonic gel[15] by fixing the metastable SiO_2 CCA in the matrix of ethylene glycol (EG) and poly(ethylene glycol) methacrylate (PEGMA) through photo-polymerization. The invisible patterns are printed on that photonic gel by soaking the whole paper with poly(ethylene glycol) diacrylate (PEGDA) and subsequently crosslinking the unshielded region in a typical photo lithography process. Since the crosslinking causes slight change in reflection wavelength between the illuminated and shielded section, the patterns are hard to be distinguished in relaxed condition. However, as the

S. Y. Ye, Q. Q. Fu, Prof. J. P. Ge
Shanghai Key Laboratory of Green Chemistry and Chemical Processes
Department of Chemistry
East China Normal University
Shanghai 200062, P. R. China
E-mail: jpge@chem.ecnu.edu.cn

DOI: 10.1002/adfm.201401562

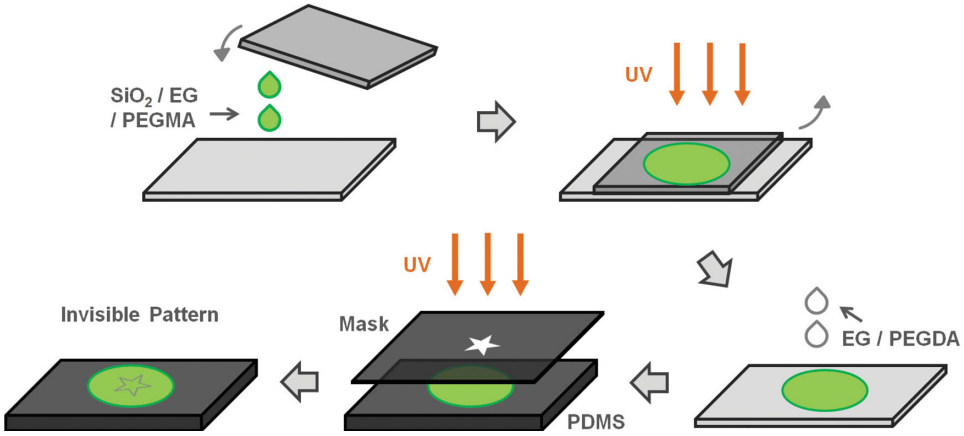

Figure 1. Schematic illustration to the printing process of invisible photonic patterns shown by deformation.

elastic photonic paper is stretched or squeezed, the different elasticity between the illuminated (crosslinked) and shielded (uncrosslinked) section will cause nonuniform deformation and thereby a large contrast of reflection wavelength, which reveals the pattern in the end. It's worth mentioning that the showing and hiding of invisible patterns are instant once the deformation is applied, and they can be reversibly achieved for many times. This new printing technique is capable of creating invisible photonic prints in both macroscale and microscale range, which makes them potentially useful for security and antifraud applications.

2. Results and Discussions

Typically, the fabrication of invisible photonic prints includes the preparation of mechanochromic photonic paper and the printing of photonic patterns on it (**Figure 1**). First of all, an elastic photonic gel was prepared by fixing the metastable SiO_2 CCA in the matrix of EG and PEGMA through photo-polymerization. The photonic gel was swelled with the mixture of EG and PEGDA, producing a monochromatic photonic paper for the following printing. Then, the patterns designed on computer were printed on a transparent slide using commercial laser printer to generate a simplified photo-mask. When the swelled photonic paper covered with photo-mask was irradiated by UV light, the exposed photonic gel would be chemically crosslinked while the shielded part would not, which produced invisible photonic prints on paper in the end. In order to improve the life time of the invisible prints, the samples were sealed inside polydimethylsiloxane (PDMS) rubber before repeated usages.

Unlike most previous colloidal crystals in polymeric materials, the elastic SiO_2/EG-PEGMA photonic paper is actually composed of microscale SiO_2 colloidal crystals and amorphous stacking of SiO_2 particle. Optical microscope image shows that it contains numerous SiO_2 colloidal microcrystals with diameters ranging from 20 to 80 μm, which strongly reflects green light in sight (**Figure 2**). The ordered arrangement of SiO_2 particles in photonic paper is also verified by the SEM images of the dried SiO_2/EG-PEGMA photonic gel, where the removal of EG does not change the order degree of colloidal assembly. The gaps between colloidal microcrystals are amorphous stacking of SiO_2 particles, because these transparent "glass" particles scarcely reflect the visible light. The coexistence of crystalline and amorphous SiO_2 is believed to inherit from the liquid precursor where only part of the particles precipitate to form metastable CCA and rest of them are randomly dispersed in the monomer before the polymerization. Since the amorphous SiO_2 will neither contribute to the reflection signals nor interfere with the SiO_2 colloidal crystals to decrease their order

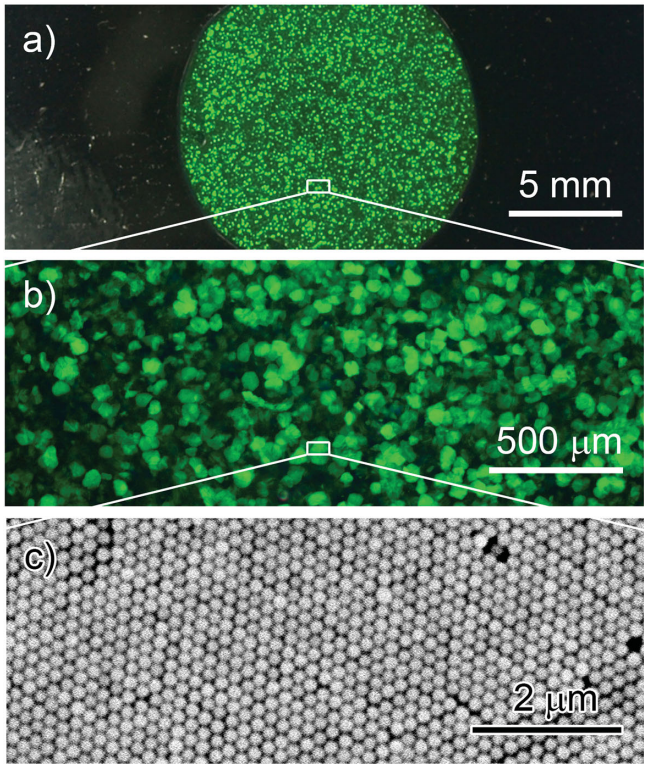

Figure 2. a) Digital photo and b) microscope image of silica colloidal microcrystals inside a SiO_2/EG-PEGMA photonic gel. c) SEM image of silica assemblies in PEGMA matrix after removing EG.

degree, the aforementioned transformation from metastable CCA to polymerized CCA is actually an efficient method to prepare high quality photonic paper in a large scale.

In order to fulfill the requirement of showing patterns by deformation, the original photonic paper must have good mechanochromic response. Benefit from the recent development of metastable colloidal crystals, the as-prepared SiO_2/EG-PEGMA photonic paper has high volume fraction of nonvolatile organic solvent (EG), which greatly improves the gel's elasticity and thereby the sensitivity of structure color to the deformation.[15] A total 150-nm reflection wavelength shift can be achieved by stretching and squeezing, which means the color change may cover the entire visible range. Meanwhile, the photonic gel also possesses a fast and reversible mechanochromic response with stable reflection intensities, all of which makes it an ideal candidate for the photonic paper required in this work.

The key point of creating invisible photonic prints is the spatial control of photonic structures with close initial optical signals but nonuniform response to external stimuli. In this specific case, we are looking for a pair of photonic structures, which will present different deformation and structural color by a same external force. Since the elasticity of a polymeric gel can usually be controlled by its chemical crosslinking level, the printing may convert to a process of producing neighboring photonic gels with different crosslink level on the paper. As the original photonic paper has no chemical crosslinking at all, it is convenient to control its level by introduce crosslinker (PEGDA) to certain part of the paper followed by a UV curing treatment.

According to the above strategy, we print a simple invisible pattern composed of two semicircles on the elastic photonic paper (**Figure 3**). The left semicircle is crosslinked by PEGDA and presents "hard" characteristics, while the right one keeps uncrosslinked and retains the "soft" feature of original paper due to the shielding of photo-mask in UV curing process. In the relax state, two semicircles are hidden due to the close reflection wavelength and similar structural color. However, when the sample is squeezed, the "soft" (right) semicircle turns red due to the expansion of crystal lattice in vertical orientation, while the "hard" (left) semicircle barely deforms and keeps on

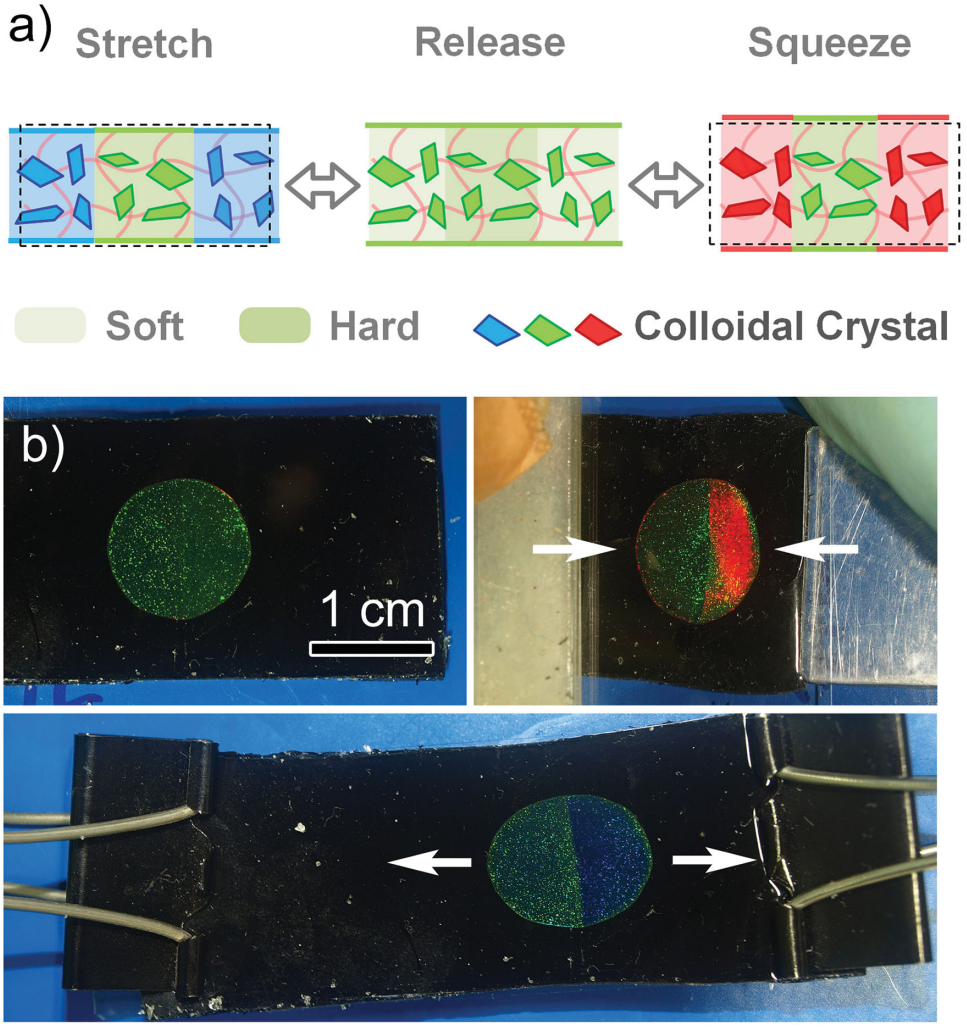

Figure 3. a) Mechanism of invisible photonic prints shown by deformation. b) Two combined semicircles are hidden in relaxed state and shown by squeezing or stretching.

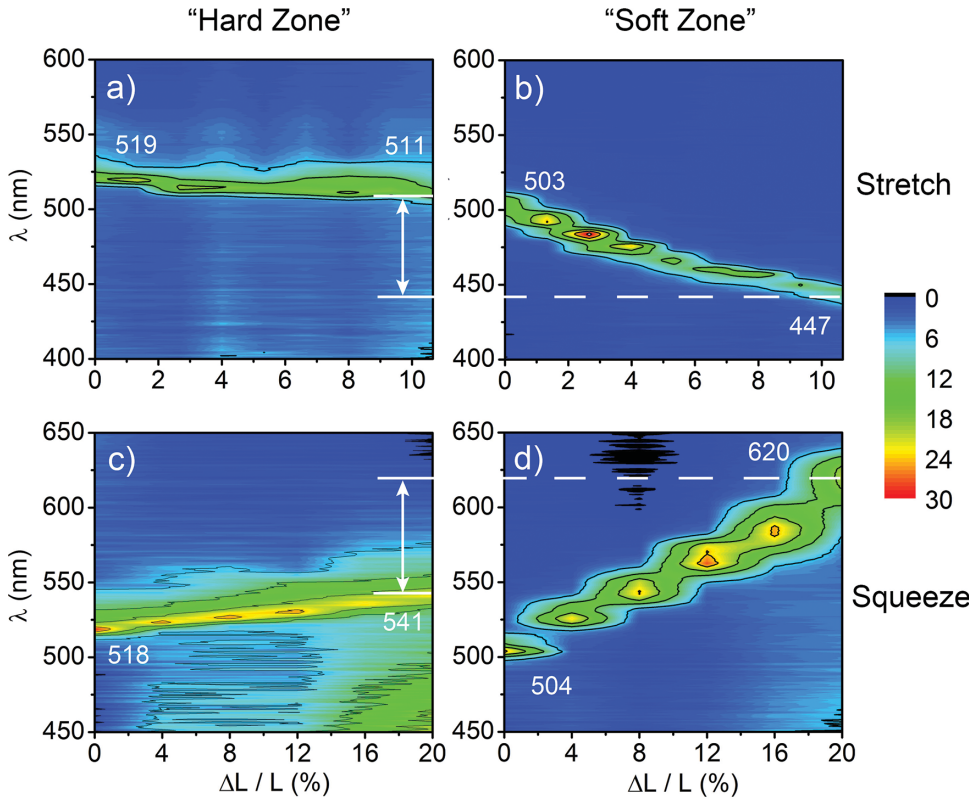

Figure 4. Color-filled contour map showing the evolution of reflection signals for crosslinked (hard) and uncrosslinked (soft) semicircles under deformation, which are printed on a photonic paper swelled by PEGDA and EG (5:5).

showing green, which forms a large contrast in color immediately. When it is horizontally stretched, the "soft" part turns blue due to the compression of crystal lattice and the "hard" one keeps unchanged, which eventually generate a visual contrast either.

The evolution of reflection spectra of two semicircles under deformation is recorded to verify the visual observation and explain the mechanism of invisible photonic prints. Here, the semicircle patterns are printed on a photonic paper swelled by PEGDA and EG mixed in volume ratio of 5:5. A three-dimensional color-filled contour map with deformation ratio in x-axis, reflection wavelength in y-axis and reflection intensities in color is used to reveal the samples' response to deformation (**Figure 4**). Taking the stretching experiment as an example, the crosslinked (hard) semicircle has a λ of 519 nm in the relaxed state, while the uncrosslinked (soft) one has a λ of 503 nm. It shows that the crosslinking causes slight change to the reflection wavelength, so that the patterns are hard to be distinguished. However, as the whole photonic paper is stretched for 10.67%, the reflection peak of crosslinked and uncrosslinked semicircle nonuniformly blue-shifts to 511 and 447 nm respectively due to relatively small and large deformation ratio, which leads to a $\Delta\lambda$ of 64 nm and a large color contrast between them finally. In fact, the entire deformation is nonuniformly distributed to the "hard" and "soft" semicircles. The deformation ratio of the former is lower than the average ratio and that of the latter is higher than the average, which induces different deformation ratios and distinct reflection wavelength shift. For the case of squeezing, a reflection wavelength contrast of 14 nm is presented between two semicircles before deformation, and it amplifies to 79 nm after the sample is squeezed for 20%, which leads to a similar hiding in release and showing under deformation. The relationship between the strain/stress applied to the PDMS substrate and the deformation ratio of the invisible photonic prints are supplied in the Supporting Information (SI, Figure S1), so that one can estimate how much force is needed to show the invisible photonic patterns. It should be noted that the green region around 450–500 nm on the contour map (when the squeezing ratio reached 20%) was caused by the rise of spectrum base line due to small distorting of photonic paper under deformation. It does not represent a new mode in photonic band gap.

The chemical crosslinking level on the photonic paper, which is controlled by the PEGDA/EG ratio during swelling, has critical influence upon the hiding and showing performance of the invisible photonic prints (**Figure 5**). In the stretching experiments (**Table 1**), we studied this relationship by comparing the reflection wavelength contrast between two semicircles before (λ_{h0}–λ_{s0}) and after ($\lambda_{h'}$–$\lambda_{s'}$) stretching, and their individual λ change (λ_{h0}–$\lambda_{h'}$; λ_{s0}–$\lambda_{s'}$) during the deformation. It should be noted that with the PEGDA/EG ratio increased from 5:5 to 7:3, the introduction of crosslinker actually decreases probably because PEGDA is harder to diffuse into the photonic gel compared to EG. Therefore, the reflection wavelength contrast before stretching (λ_{h0}–λ_{s0}) decreases from 16 to 4 nm, which proves a low introduction of crosslinker and a small change to

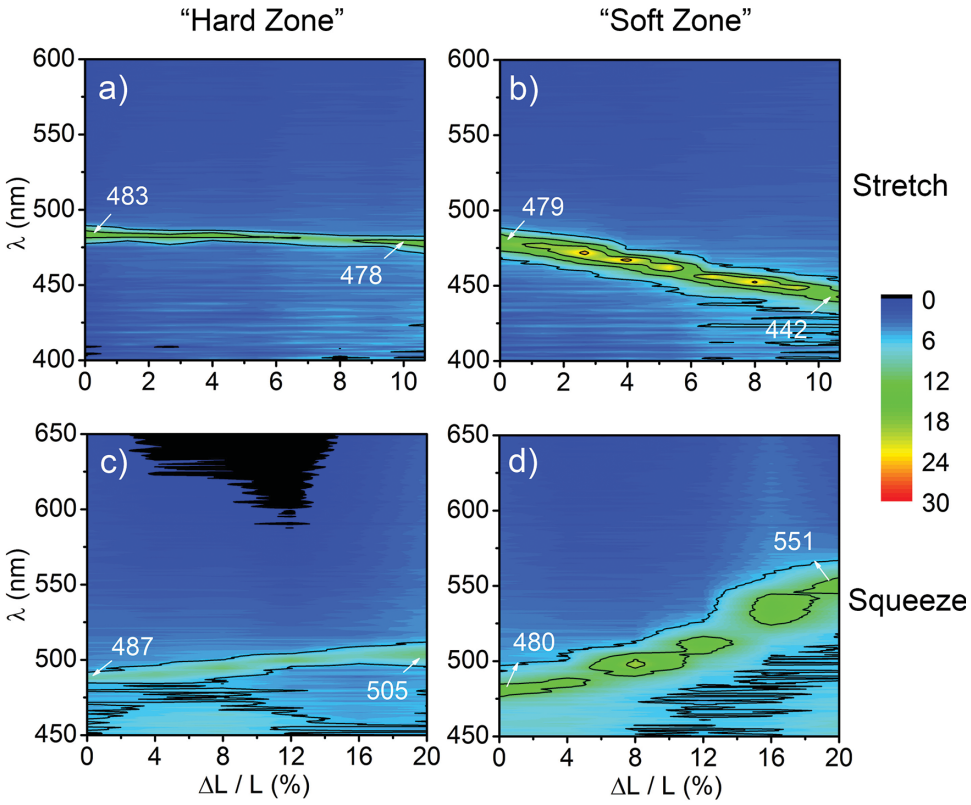

Figure 5. Color-filled contour map showing the evolution of reflection signals for crosslinked (hard) and uncrosslinked (soft) semicircles under deformation, which are printed on a photonic paper swelled by PEGDA and EG (7:3).

photonic structure. Although the introduction of crosslinker does not change the elasticity or mechanochromic property of the shielded (uncrosslinked) semicircle directly, its practical deformation ratio is indirectly affected by the crosslinking level of the neighboring semicircle. Because the higher crosslinking level is created in the "hard" semicircle, the larger deformation will be distributed to the "soft" semicircle when the entire stretching ratio is kept the same (10.66%). That explains the λ change of uncrosslinked semicircle (λ_{s0}–$\lambda_{s'}$) decreases from 56 to 37 nm as the crosslinking decreases. Therefore, the final reflection wavelength contrast after stretching ($\lambda_{h'}$–$\lambda_{s'}$) decrease from 64 to 36 nm accordingly. Similar trends can be concluded in the squeezing experiments (**Table 2**). Both results prove that a lower crosslinking level favors the hiding of invisible patterns before deformation and a higher crosslinking level favors the showing of patterns after deformation. Currently, the PEGDA/EG ratio of 5:5 is the optimized recipe for the best hiding and showing performance.

Table 1. Reflection wavelength contrast between the crosslinked (hard) and uncrosslinked (soft) semicircles before (λ_{h0}–λ_{s0}) and after ($\lambda_{h'}$–$\lambda_{s'}$) stretching (10.67%), and their individual λ change (λ_{h0}–$\lambda_{h'}$, λ_{s0}–$\lambda_{s'}$) along with the deformation

PEGDA : EG	λ_{h0}–$\lambda_{h'}$ [nm]	λ_{s0}–$\lambda_{s'}$ [nm]	λ_{h0}–λ_{s0} [nm]	$\lambda_{h'}$–$\lambda_{s'}$ [nm]
5 : 5	8	56	16	64
7 : 3	5	37	4	36

Table 2. Reflection wavelength contrast between the crosslinked (hard) and uncrosslinked (soft) semicircles before (λ_{s0}–λ_{h0}) and after ($\lambda_{s'}$–$\lambda_{h'}$) squeezing (20%), and their individual λ change ($\lambda_{h'}$–λ_{h0}, $\lambda_{s'}$–λ_{s0}) along with the deformation.

PEGDA : EG	$\lambda_{h'}$–λ_{h0} [nm]	$\lambda_{s'}$–λ_{s0} [nm]	λ_{s0}–λ_{h0} [nm]	$\lambda_{s'}$–$\lambda_{h'}$ [nm]
5 : 5	23	116	–14	79
7 : 3	18	71	–7	46

The as-prepared photonic printing can reversibly show its patterns by deformation and hide themselves by releasing for many times. Two samples made from same SiO_2 particles are used to prove the reversibility in squeezing and stretching, respectively. **Figure 6** shows the reflection wavelength and intensity change of the "hard" crosslinked semicircle (by black squares) and the "soft" uncrosslinked semicircle (by red circles) in 10 continuous squeezing-releasing and stretching-releasing operations. Here, the ratio of squeezing and stretching are 16% and 6.67%, respectively. For cycling squeezing-releasing experiment, the reflection wavelength of two semicircles approximately remains unchanged in every relaxed and deformed state. At the same time, in each cycle, the originally small reflection wavelength contrast in relaxation state between two semicircles always enlarges by squeezing and recovers immediately by relaxation. Furthermore, the reflection intensities increase by squeezing and recover by relaxation, and they also present

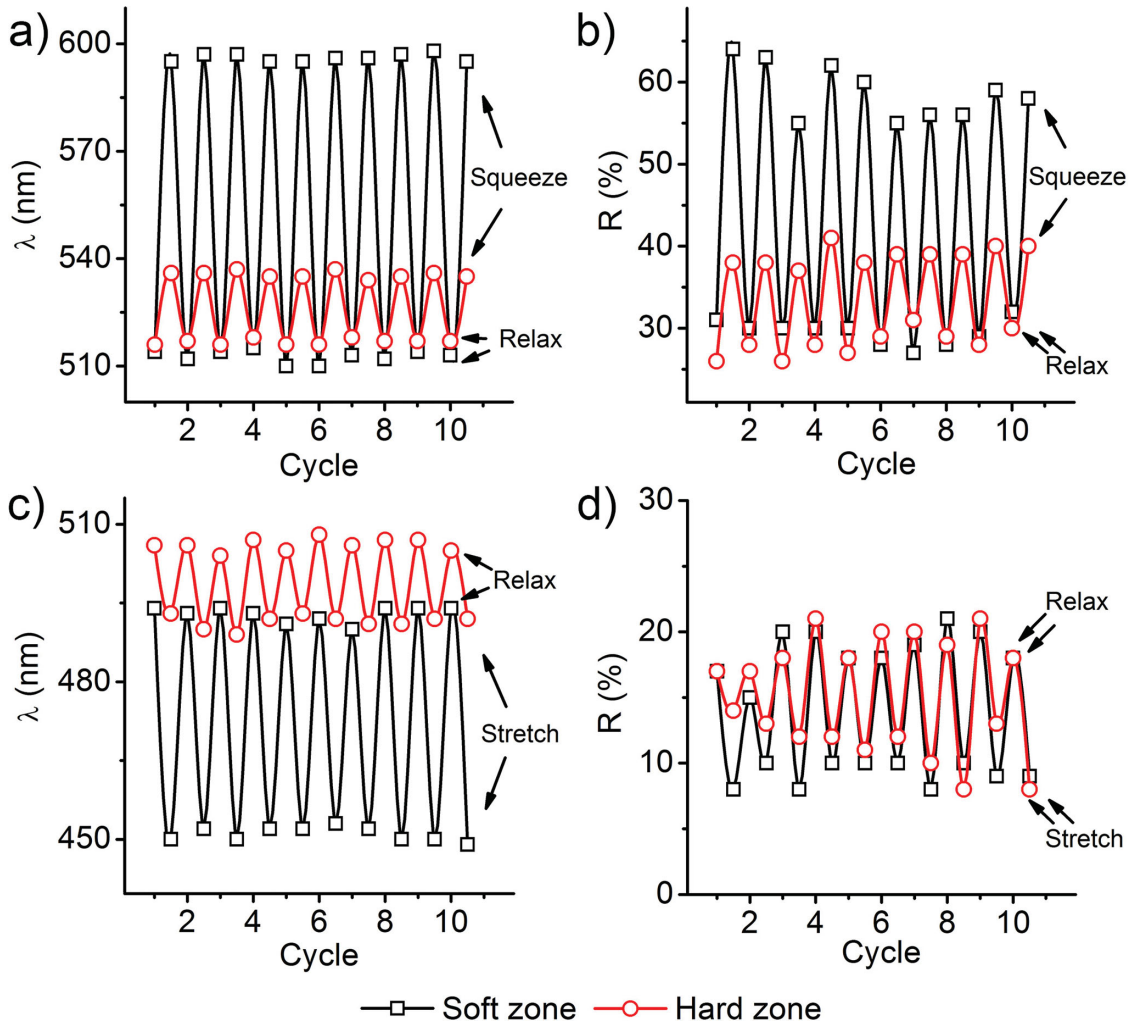

Figure 6. a,c) Reflection wavelength and b,d) intensity change for the crosslinked (hard) and uncrosslinked (soft) semicircle in 10 continuous a,b) squeezing-releasing and c,d) stretching-releasing tests.

periodical characteristics during the test. All these results prove that showing and hiding of invisible photonic prints can be instantly and reversibly realized by squeezing and releasing. For stretching experiments, similar reversibility can be concluded except for a relatively large fluctuation in the reflection intensity. In experiment, invisible photonic prints encapsulated in PDMS rubber are repeatedly squeezed and released for 100 times, and its showing-hiding function works well in all the cycles. (SI, Figure S2) According to our experience, this reversibility can be maintained unless the photonic gel breaks into pieces by over deformation or loses the mechanochromic effects due to EG evaporation.

In order to prolong the life time and enhance the durability of the invisible photonic prints in practical usage, they are encapsulated in polydimethylsiloxane (PDMS) after the printing process. Generally, the deformation ratio in practical usage is smaller than the maximum value that the photonic gel can bear (12% for stretching and 22% for squeezing), because an adequately large $\Delta\lambda$ has already been achieved. But the elastic gel still has a risk of cracking when the deformation exceeds its critical value accidently. A transparent and elastic PDMS rubber with better mechanic strength and larger deformation range will protect the gel from breaking in most cases. Furthermore, it can slow the evaporation of EG, so that the invisible photonic prints can be kept at room temperature for a month without losing the normal functions. The PDMS encapsulation also renders the photonic prints good durability for long term deformation. In a fatigue test composed of 3 consecutive stretching-releasing processes, where the photonic prints are continuously stretched for 1 hour before being released (**Figure 7**), the reflection wavelengths of both the crosslinked and uncrosslinked semicircle change instantly with the deformation and show periodical changes, which proves that the invisible photonic prints work fine even after long time deformation and it is ready for daily usages.

As a demonstration, invisible photonic prints of "sunlight" and "rabbit" are printed by the new printing method. (**Figure 8**; SI, Figure S3) These patterns are invisible under normal conditions. When the samples are squeezed, the background turns red and the patterns keep green, so that the hidden images are revealed. Showing by stretching is similar except that the color contrast is formed by the green pattern and blue background in

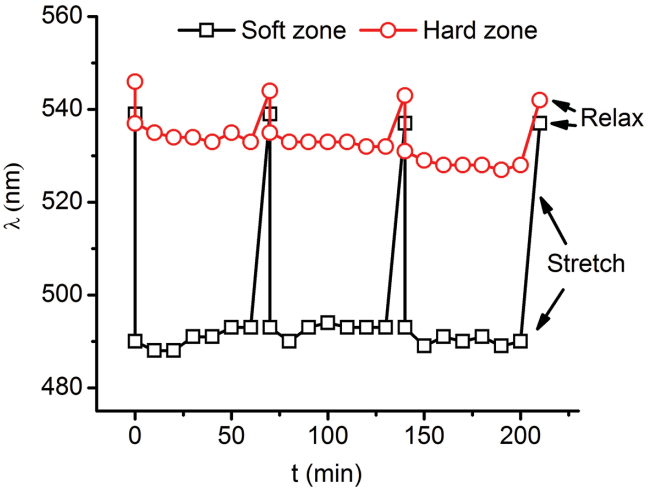

Figure 7. Reflection wavelength change for the crosslinked and uncrosslinked semicircle in a fatigue test, where the sample is stretched for about 60 min in each cycle.

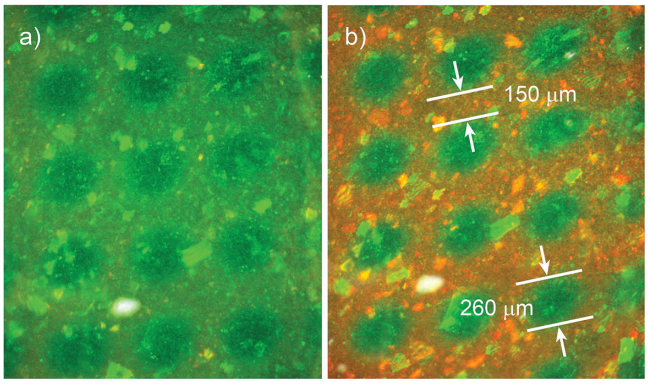

Figure 9. Microscale invisible photonic prints of orthogonally arranged circular array shown by squeezing.

that case. It should be noted that the latter visual effect is realized by pushing and slight bending the sample with its convex surface facing up, because such bending causes same change in crystal lattice as the horizontal stretching. (SI, Figure S4) Although the sample is slightly bended, the small distorting of photonic gel is unable to cause large color change, (SI, Figure S5) so that deformation is the only factor to trigger the change of structural colors in this work. A perfect invisibility can be achieved only if the infiltration and crosslinking of PEGDA are appropriate. A long time soaking (3–4 h) by the mixture of PEGDA and EG leads to introduction of high level PEGDA, which raises the refractive index of polymer matrix to be close to that of silica. (n_{PEGDA} = 1.47; n_{EG} = 1.431; n_{PEGMA} = 1.464; n_{SiO2} = 1.46) The match of refractive index turns the photonic crystals to be transparent even if the ordered structures are maintained, which makes the photonic patterns hard to be invisible in normal relaxed state. (SI, Figure S6)

The printing of invisible photonic patterns can be extended to microscale range by using a more sophisticated photo mask to achieve higher resolution. Here, a 60 mesh stainless steel grid was used as photo mask to print orthogonally arranged circular array on the green photonic paper (**Figure 9**). In the beginning, the circular array and the gaps have similar structural color so that the patterns are "invisible" in the relaxation state. It must be admitted that the microscopic image reveals the tiny difference between the patterns and the background due to high sensitivity of CCD camera. The gaps are composed of photonic gel swelled by liquid mixture of PEGDA and EG, which makes them some sort of yellowish in dark-field reflection mode. While the circular array is composed of crosslinked photonic

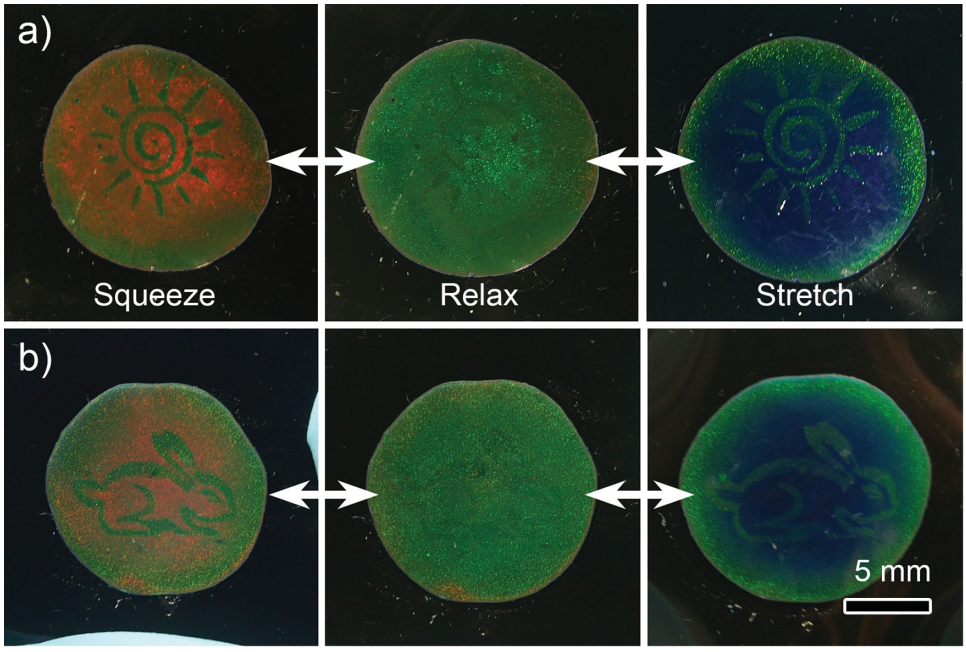

Figure 8. Invisible photonic prints of a) sunlight and b) rabbit hidden in relaxed state and shown by deformation.

gel, so that it looks greenish in microscope compared to the gap region. When the prints are squeezed, the structural colors of the gap region turns red immediately due to mechanochromic effect, while that of the circular region remains green because of the crosslinking, which generate a large color contrast to reveal the invisible patterns. Once the squeezing is released, the circular array changes back to invisible state, and the switching is fully reversible. Considering the circular pattern has a diameter of 260 μm and the interspacing between circles is 150 μm, an even higher resolution may be accomplished with better photo mask and optimization of printing process.

3. Conclusion

In summary, invisible photonic prints shown by deformation are prepared by soaking the mechanochromic photonic paper with crosslinker PEGDA and subsequently curing part of the paper through a photo lithography process. A mechanochromic photonic paper with sensitive, fast and reversible response to the external forces is a fundamental requirement for the fabrication of invisible photonic prints. The key point of this new printing technique is preparing patterns whose mechanochromic property is different from that of the background on the elastic photonic paper, so that a nonuniform change in photonic structure will be realized under deformation. Meanwhile, a structural difference as small as possible between the pattern and background is also demanded in relaxation state for the invisible purpose. Based on the relationship between crosslinking level and the reflection changes during deformation, one can conclude that a lower crosslinking level favors the hiding of invisible patterns before deformation and a higher crosslinking level favors the showing of patterns after deformation. With the optimization of crosslinking level, the patterns and the background will have a small $\Delta\lambda$ (5–15 nm) in the relaxed state but a much larger $\Delta\lambda$ (60–80 nm) under deformation. The as-prepared samples can instantly and reversibly show the patterns by deformation and hide them by relaxation for many times, and the encapsulation by PDMS rubber prolongs the life time and enhances the durability of the sample in fatigue test. This new printing technique is capable of creating invisible photonic prints in both macroscale and microscale range, which makes them potentially useful for antifraud labels and identity recognition in our future life.

4. Experimental Section

Materials: Tetraethylorthosilicate (TEOS, 98%), aqueous ammonia (28%) were purchased from Sinopharm Chemical Reagent Co. Ltd. Carbon black (99.5%, 30 nm) was purchased from Aladdin Co. Ltd. Ethylene glycol (EG, 99%) and ethanol (99.9%) were purchased from J&K Co. Ltd. Poly(ethylene glycol) methacrylate (PEGMA, Mn = 360) and Poly(ethylene glycol) diacrylate (PEGDA, Mn = 700) was purchased from Sigma-Aldrich. Silicone elastomer base and curing agent (Sylgard 184) were obtained from Dow Corning. All chemicals were used directly as received without further purification.

Preparation of Photonic Crystal Paper: In a typical process, an elastic SiO_2/EG-PEGMA photonic paper was prepared by fixing the metastable SiO_2 CCA in the matrix of EG and PEGMA through photo-polymerization. Monodisperse SiO_2 particles with a diameter of ≈190 nm were first synthesized by Stöber method. SiO_2 particles (0.08 cm^3) dispersed in ethanol (1.0 mL) were mixed with EG (77 μL) and PEGMA (43 μL). It was concentrated to a solution of 200 μL by heating at 90 °C for 2 h. After being cooled down to room temperature, 30 μL of the liquid suspension was sandwiched between two glass slides separated by an interval of 0.18 mm and placed without disturbance for 10 min to form a metastable CCA precursor, which was further cured by UV light (365 nm, 4.8 mW/cm^2) for 20 min to generate a mechanochromic photonic paper.

Printing the Invisible Pattern: The photonic paper was soaked with the mixture of PEGDA and EG (5:5 or 7:3, 30 μL) for 2 h, peeled off by a razor blade and transferred onto a carbon nano-powder doped polydimethylsiloxane (PDMS) rubber with thickness of 2 or 4 mm. Here, PDMS rubber was prepared by mixing the silicone elastomer prepolymer, curing agent and carbon powders in a mass ratio of 20:2:1 and curing at 60 °C for 1 h. The soaked paper was covered by a photo mask, and exposed to UV light for 25 s to generate invisible photonic patterns. After removing the photo mask, the photonic paper was covered by a premade transparent PDMS rubber and sealed by curing the additionally added silicone elastomer prepolymer at 60 °C for 50 min. The as-made sample is kept at room temperature for the following measurements and characterizations.

Characterization: The reflection spectra were measured by an Ocean Optics Maya 2000 Pro fiber spectrometer coupled to a six-around-one reflection/back scattering probe, where both the incident and reflective angle were fixed at 0°. Generally, the optical probe collected reflection signals of a circular region with a diameter of about 4 mm. Therefore, all reflection spectra are measured at the center of two semicircles considering the diameter of the circular sample is only 10–12 mm. The optical microscope images were taken by an Olympus BXFM reflection-type microscope operated in dark-field mode. The assembly of silica colloids within the photonic crystals paper was observed by a Phenom G2 Pro scanning electron microscope.

Supporting Information

Supporting Information is available from the Wiley Online Library or from the author.

Acknowledgements

J.P.G. thanks National Science Foundation of China (21222107), Shanghai Rising-Star Program (13QA1401400) and Youth Talent Plan (Organization Department of the Central Committee of the CPC) for support.

Received: May 15, 2014
Revised: July 3, 2014
Published online: August 19, 2014

[1] C. I. Aguirre, E. Reguera, A. Stein, *Adv. Funct. Mater.* **2010**, *20*, 2565–2578.

[2] a) J. M. Weissman, H. B. Sunkara, A. S. Tse, S. A. Asher, *Science* **1996**, *274*, 959–960; b) S. Kubo, Z. Z. Gu, K. Takahashi, A. Fujishima, H. Segawa, O. Sato, *J. Am. Chem. Soc.* **2004**, *126*, 8314–8319; c) Y. F. Yue, M. A. Haque, T. Kurokawa, T. Nakajima, J. P. Gong, *Adv. Mater.* **2013**, *25*, 3106–3110; d) E. P. Chan, J. J. Walish, E. L. Thomas, C. M. Stafford, *Adv. Mater.* **2011**, *23*, 4702–4706; e) J. P. Ge, Y. X. Hu, Y. D. Yin, *Angew. Chem. Int. Ed.* **2007**, *46*, 7428–7431.

[3] a) J. H. Holtz, S. A. Asher, *Nature* **1997**, *389*, 829–832; b) M. Honda, T. Seki, Y. Takeoka, *Adv. Mater.* **2009**, *21*, 1801–1804; c) Z. H. Wang, J. H. Zhang, J. Xie, C. A. Li, Y. F. Li, S. Liang, Z. C. Tian, T. Q. Wang,

H. Zhang, H. B. Li, W. Q. Xu, B. Yang, *Adv. Funct. Mater.* **2010**, *20*, 3784–3790; d) R. A. Potyrailo, H. Ghiradella, A. Vertiatchikh, K. Dovidenko, J. R. Cournoyer, E. Olson, *Nat. Photonics* **2007**, *1*, 123–128; e) Y. N. Wu, F. T. Li, W. Zhu, J. C. Cui, C. A. Tao, C. X. Lin, P. M. Hannam, G. T. Li, *Angew. Chem. Int. Ed.* **2011**, *50*, 12518–12522; f) C. F. Blanford, R. C. Schroden, M. Al-Daous, A. Stein, *Adv. Mater.* **2001**, *13*, 26–29.

[4] a) Y. J. Zhao, X. W. Zhao, J. Hu, J. Li, W. Y. Xu, Z. Z. Gu, *Angew. Chem. Int. Ed.* **2009**, *48*, 7350–7352; b) M. Z. Li, F. He, Q. Liao, J. Liu, L. Xu, L. Jiang, Y. L. Song, S. Wang, D. B. Zhu, *Angew. Chem. Int. Ed.* **2008**, *47*, 7258–7262; c) J. T. Heeres, S. H. Kim, B. J. Leslie, E. A. Lidstone, B. T. Cunningham, P. J. Hergenrother, *J. Am. Chem. Soc.* **2009**, *131*, 18202–18203.

[5] a) A. C. Arsenault, D. P. Puzzo, I. Manners, G. A. Ozin, *Nat. Photonics* **2007**, *1*, 468–472; b) I. Lee, D. Kim, J. Kal, H. Baek, D. Kwak, D. Go, E. Kim, C. Kang, J. Chung, Y. Jang, S. Ji, J. Joo, Y. Kang, *Adv. Mater.* **2010**, *22*, 4973–4977.

[6] a) A. C. Arsenault, T. J. Clark, G. Von Freymann, L. Cademartiri, R. Sapienza, J. Bertolotti, E. Vekris, S. Wong, V. Kitaev, I. Manners, R. Z. Wang, S. John, D. Wiersma, G. A. Ozin, *Nat. Mater.* **2006**, *5*, 179–184; b) I. B. Burgess, L. Mishchenko, B. D. Hatton, M. Kolle, M. Loncar, J. Aizenberg, *J. Am. Chem. Soc.* **2011**, *133*, 12430–12432; c) H. S. Lee, T. S. Shim, H. Hwang, S. M. Yang, S. H. Kim, *Chem. Mater.* **2013**, *25*, 2684–2690.

[7] a) J. R. Lawrence, Y. R. Ying, P. Jiang, S. H. Foulger, *Adv. Mater.* **2006**, *18*, 300–303; b) H. Li, J. X. Wang, H. Lin, L. Xu, W. Xu, R. M. Wang, Y. L. Song, D. B. Zhu, *Adv. Mater.* **2010**, *22*, 1237–1241.

[8] a) Y. Lu, H. T. Yu, S. Chen, X. Quan, H. M. Zhao, *Environ. Sci. Technol.* **2012**, *46*, 1724–1730; b) M. Zhou, H. B. Wu, J. Bao, L. Liang, X. W. Lou, Y. Xie, *Angew. Chem. Int. Ed.* **2013**, *52*, 8579–8583.

[9] a) A. Mihi, C. J. Zhang, P. V. Braun, *Angew. Chem. Int. Ed.* **2011**, *50*, 5711–5714; b) S. Colodrero, A. Forneli, C. Lopez-Lopez, L. Pelleja, H. Miguez, E. Palomares, *Adv. Funct. Mater.* **2012**, *22*, 1303–1310.

[10] a) J. G. McGrath, R. D. Bock, J. M. Cathcart, L. A. Lyon, *Chem. Mater.* **2007**, *19*, 1584–1591; b) L. Y. Cui, Y. F. Li, J. X. Wang, E. T. Tian, X. Y. Zhang, Y. Z. Zhang, Y. L. Song, L. Jiang, *J. Mater. Chem.* **2009**, *19*, 5499–5502; c) H. Kim, J. Ge, J. Kim, S. Choi, H. Lee, H. Lee, W. Park, Y. Yin, S. Kwon, *Nat. Photonics* **2009**, *3*, 534–540; d) S. H. Kim, S. M. Yang, *Adv. Mater.* **2009**, *21*, 3771–3775.

[11] a) H. Fudouzi, Y. N. Xia, *Adv. Mater.* **2003**, *15*, 892–896; b) P. Jiang, D. W. Smith, J. M. Ballato, S. H. Foulger, *Adv. Mater.* **2005**, *17*, 179–184; c) R. Y. Xuan, J. P. Ge, *Langmuir* **2011**, *27*, 5694–5699.

[12] R. Y. Xuan, J. P. Ge, *J. Mater. Chem.* **2012**, *22*, 367–372.

[13] H. B. Hu, J. Tang, H. Zhong, Z. Xi, C. L. Chen, Q. W. Chen, *Sci. Rep.* **2013**, *3*, 1484.

[14] D. P. Yang, S. Y. Ye, J. P. Ge, *J. Am. Chem. Soc.* **2013**, *135*, 18370–18376.

[15] D. P. Yang, S. Y. Ye, J. P. Ge, *Adv. Funct. Mater.* **2014**, 24.